Proceedings of the 2nd EAA International Symposium on Hydroacoustics
24-27 May 1999, Gdańsk-Jurata
POLAND

Thermal Cavitation Mechanism for Generation of Underwater Sound

S. Buogo, G. B. Cannelli

CNR - Istituto di Acustica "O. M. Corbino"
Underwater Acoustics Laboratory
Via del Fosso del Cavaliere 100, 00133 Roma, Italy
e-mail: silvano@idac.rm.cnr.it

The implosion of a vapour bubble generated by spark discharges in seawater can generate high power pulses in the frequency band up to a few hundred kHz, useful to obtain high-resolution imaging of the sea subbottom. In this paper, a physical model is illustrated to explain the origin of the process generating the bubble in a conducting liquid, together with a brief review of the hypothized ideas on the growth and implosion mechanism of the bubble. A description is given of the implementation of a numerical scheme for the solution of a set of equations describing the temperature and electric field distributions in the liquid in the prebreakdown stage. According to this model, electrical breakdown and subsequent thermal cavitation in seawater is governed by Joule heating with a temperature dependent electrical conductivity. Measurements of the discharge of the paraboloidal sparker-based source confirm the validity of the energy model, showing a good agreement of the predicted time required for liquid vaporization with the observed breakdown time.

1. Introduction

Thermal cavitation is meant here as a mechanism of bubble generation in a fluid where thermal effects dominate, rather than inertial. Plesset and Prosperetti employed preferably the term "vapour bubble", as opposed to "cavitation bubble", when describing the dynamics of vapour cavities in similar cases [1]. Bubble generation by an underwater spark is a typical example of phenomenon where thermal effects play the leading role. Sparkers have been more and more used in the past decades to generate underwater high-power pressure pulses as a convenient alternative to explosives. Recently, at the Istituto di Acustica "O. M. Corbino" (IDAC), significant advances have been made in their technology by using paraboloidal sparker-based sources [2]. These sources are more versatile than traditional ones, being adaptable to different applications in a range of low and middle frequency band not available in traditional sonar devices. Exploiting the implosion of a vapour bubble, generated by the sparker discharge at the paraboloid focus, this type of source can generate high power pulse in the band centered around some hundred kHz, useful to obtain a high-resolution imaging of the near surface anomalies and objects of the sea subbottom [3]. This latter unique feature stimulates further investigation on the bubble phenomenon both from a theoretical and experimental point of view. The starting point is to investigate the genesis of the vapour bubble, namely the physical processes occurring during the pre-breakdown and breakdown phases of the electrical discharge. The process of electrical discharge in water has found some interest in the seventies when a number of investigations based mainly on optical techniques aimed at explaining the nature of breakdown and prebreakdown phenomena [4,5]. A difference in behaviour was found between dielectric liquid and conducting liquid. Pulsed discharges in dielectric liquids were shown to initiate with the development of a leader, that is a plasma channel starting from one of the electrodes [6,7]. Breakdown was seen to occur in plasma and not in the liquid, as the consequence of the formation of an arc when the channel bridges the electrode gap. The leader growth from electrode to electrode in the prebreakdown phase was found to be dependent on the electrical conductance of the liquid, and was absent in low resistance electrolytes such as salt water at large concentrations. From these early

observations it was argued that the principal role for the onset of breakdown in this latter liquid could be played by thermal processes [8]. In such cases an electric arc develops in a bubble filled with electrolytic gas and water vapour near one of the electrodes. This bubble is due to vaporization, caused by the large electric current flowing in the liquid.

In this paper, a physical model is illustrated to explain the origin of the process generating the bubble in a conducting liquid, together with a brief review of the hypothized ideas on the growth and implosion mechanism of the bubble. This study is crucial in view of improving the performance of the innovative paraboloidal sparker source.

2. Thermal Cavitation in a Conducting Liquid

Very few investigations have been made on the genesis of the vapour bubble process. An attempt to develop a numerical model of the electrical discharge in a conducting liquid was made to find the temperature and electric field perturbations during the preleader stage for the particular case of concentric spherical electrodes and infinite source capacity [9]. The duration of the preleader and leader stage of the discharge was observed to depend on the applied voltage and the electrical conductivity of the liquid, the latter being a function of temperature. As a consequence, the development of thermal instability in the liquid was proposed as the initiating mechanism of the discharge. As a confirmation of the validity of a thermal model, an experimental study showed that breakdown in seawater is strictly correlated with vaporization [10]. Although vaporization could not be observed directly, a threshold energy was determined based on the minimum energy required to observe a bubble collapse pulse in the acoustic signature. Breakdown was shown to take place only after this threshold energy has been dissipated in the liquid. The proposed model for breakdown in seawater based on vaporization showed to be consistent up to field strengths of 50 kV/cm. An open question remains on how large a vapour bubble must grow to initiate breakdown, and whether the dielectric strength of the liquid plays an essential role in the process.

High-power sparkers generate a lot of bubbles, due to the extremely high rate of energy transfer in a little portion of liquid. In these sources, a typical energy of several hundred Joule is dissipated in less than 1 ms inside a volume of the order of 1 cm^3, which gives a mean energy density of the order of 1 MW/cm^3. A large portion of this energy is transferred to the liquid after breakdown time, causing a violent expansion of the plasma channel due to the very large electric current (order of kA) flowing in it. This causes the first shock wave travelling in the liquid, that is recorded as the primary pressure pulse in the acoustic signature of the source. It was argued in previous preliminary studies [11,12] that following this violent outward motion, an inertial expansion may bring a vapour bubble to a maximum radius, after which the motion is reversed and a collapse is started. The bubble dynamics is slow enough so that no acoustic wave is generated. At the end of the collapse phase, when condensation of vapour inside the bubble cannot compensate for the decrease of the bubble volume, the liquid motion is suddenly stopped and another shock wave is generated. Vapour inside the bubble may contain residual non-condensable gas, and one or more rebound may take place after the first collapse. More controlled pulses are generated in the paraboloidal sparker source designed at IDAC [2]. In this source the electrodes are placed in the focal point of a paraboloidal reflector, to provide a high-intensity directional response. A rigid surface is only a few cm away from the point where cavitation occurs, and this must have some influence on bubble evolution, compared to the free field case. Indeed, the acoustic signature of the paraboloidal source shows two distinct pulses: the first one is attributed to the shock wave produced at breakdown time and the second one, occurring several ms later, is very likely due to the collapse of a single large vapour bubble. The time delay between the two pulses was seen to be increasing with the electrostatic energy, and was higher for smaller electrode gap distances. From the analysis of experimental data, a model was proposed to explain the growth and collapse of a spherical bubble under the effect of the internal vapour pressure [11]. The delay was seen to be slightly increasing with the temperature of the liquid: this variation was in good agreement with the corresponding variation of the vapour pressure of water [13]. To exploit thermal cavitation as a way to produce controlled high-power pulsed sound with the maximum acoustic efficiency, an improvement of the electromechanical part of the paraboloidal source was made that allowed the primary pulse to be minimized concentrating the acoustic energy in a very high-intensity single pulse. One possible cause for the considerably simpler acoustic signature of the paraboloidal source is the presence of the rigid surface that makes the bubble collapse with a highly asymmetric shape [14]. The surface might influence the bubble evolution after the first collapse, suppressing a subsequent rebound and oscillation. This is the objective of a research project, still in progress at IDAC, which aims to the design a novel high-power, high-resolution transducer for sea subbottom prospecting. In Fig. 1, a comparison is shown between the time signature of a traditional sparker source and that of the paraboloidal sparker for the two different prototypes: the old one and the improved one.

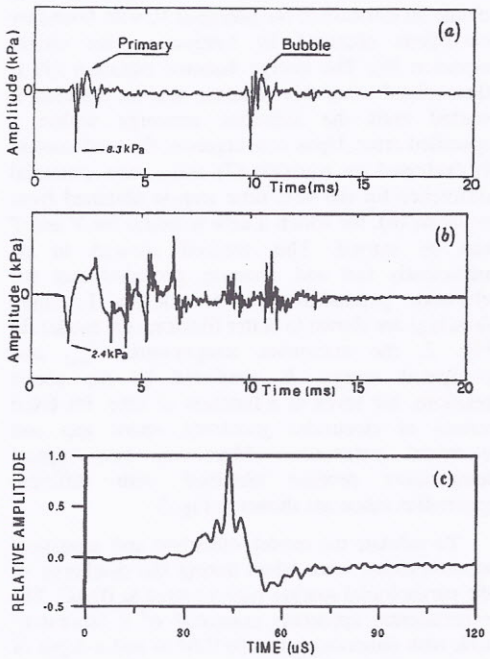

Fig. 1. Comparison among the acoustic signatures of the old prototype of paraboloidal sparker-based source (a), of a traditional sparker source (b) and of the improved paraboloidal prototype (c).

3. Analytical Approach to Breakdown Process

In recent papers, an attempt has been made to develop an analytical approach to breakdown and cavitation process in seawater [15,16]. A number of preliminary tests were done, using the paraboloidal source, to measure the characteristics of the electrical discharge and to validate some hypothesis on the involved mechanisms. One major feature that was noted experimentally, for spark discharges in seawater by paraboloidal sources, is their relatively long breakdown time (of the order of ten to hundred μs), in comparison with that found in true dielectric breakdown occurring at time scales of less than one μs. Another aspect of thermal breakdown is the considerably lower field strength with respect to that for the true dielectric breakdown: its value can be of 10-20 kV/cm only compared to many hundreds of kV/cm.

From the analysis of the voltage and current plots recorded during discharges with charge voltage 2.25 kV, energy 200 J, it was found that a considerable portion of the total electrostatic energy is transferred into heat in the discharge phase after breakdown [15]. This amount of energy is available for plasma channel expansion and subsequent vapour bubble growth, which gives an indication of the conversion efficiency of electrical energy into mechanical energy, namely the acoustic efficiency of the source.

In the following, a description is given of the implementation of a numerical scheme for the solution of a set of equations describing the temperature and electric field distributions in the liquid in the prebreakdown stage. The starting point is to evaluate how long it takes for an applied electric field to raise the liquid temperature by Joule effect up to a critic temperature when the liquid starts to vaporize. If we assume that breakdown takes place when vapour regions bridge the electrode gap, the evaluated time to reach the critic temperature should be comparable with, and no greater than, the breakdown time, that is the time delay between field application and the onset of breakdown. In the following, convective effects are neglected since the time scale is too small to allow significant motion of the liquid. Under this assumption, the process of electrical discharge can be described by Ohm's law with a temperature dependent electrical conductivity $\sigma(T)$. The statement of conservation of electric charge becomes

$$\nabla\cdot\left[\sigma(T)\nabla V\right]=0. \tag{1}$$

After some passages, this equation takes the form

$$\nabla^2 V=-\frac{1}{\sigma}\frac{d\sigma}{dT}\nabla T\cdot\nabla V, \tag{2}$$

which is a Poisson equation for the potential in the liquid to be solved with boundary conditions $\pm V(t)/2$ on the surface of the two electrodes.

The thermal power density dissipated in the liquid is given by

$$W_g=\sigma(T)\left|\nabla V(\mathbf{x})\right|^2, \tag{3}$$

and the temperature evolves according to

$$\frac{dT}{dt}=\frac{1}{\rho c_p}\left(W_g+k\nabla^2 T\right), \tag{4}$$

where ρ, c_p and k are the density, specific heat and thermal conductivity of the liquid. The conductive term in the right-hand side of eq. (4) can be shown to be much less important than the heat generation term for field strengths of 10^4 - 10^5 V/cm [9]. Therefore, boundary conditions for T in equation (4) are not critical and one can assume, for simplicity, that there is no heat exchange between the liquid and the electrodes. Due to the presence of the $\sigma(T)$ term the coupled system of eqs. (2) and (4) is non-linear. The functional form of σ is assumed to be

$$\sigma(T)=\frac{A}{T}e^{-B/T}, \tag{5}$$

where A and B are empirical constants. According to this model, breakdown is the result of an instability due to the increased electrical conductance as the temperature is raised by the flow of electric current. For a finite storage of electrostatic energy, the potential difference across the electrodes is not a constant, but varies according to the electrical parameters of the charge circuit. Assuming a simple *RLC* model, the equation giving the approximate boundary condition for Eq. (4) is

$$V = V_0 - \frac{1}{C}\int I\,dt - L\frac{dI}{dt}, \qquad (6)$$

where V_0 is the initial charge voltage of the capacitor. Here the electrode gap is assumed to be purely resistive, and the circuit resistance is neglected. This is true for the pre-breakown stage, when the gap resistance dissipates most of the electrostatic energy.

The electrical current can be evaluated by integration of the current density over a closed surface S around one of the electrodes:

$$I = \int_S \nabla V \cdot \mathbf{n}\, dS, \qquad (7)$$

where $\mathbf{n}$ is the unit vector normal to S.

Equations (2), (4), (6) and (7) form a set of coupled nonlinear equations to be solved simultaneously for T and V. Each differential equation is solved with a numerical scheme, using a bispherical coordinate transformation to map the space outside the electrodes in a rectangular space. The first step is to solve the Poisson equation (2) with initial uniform temperature and conductivity to obtain an estimate of the potential V, with boundary conditions obtained by integrating the circuit equation (6). The energy balance equation (4) is then solved using this estimate, and an iteration is started until the solutions converge within a specified error. Upon convergence, the total current is evaluated by equation (7) and a new potential difference for the next time step is obtained from equation (6), for which a new iteration for V and T can be started. This method showed to be sufficiently fast and accurate, provided that the electrode gap/radius ratio is not >> 1. Some drawings are shown to better illustrate the model. In Fig. 2, the maximum temperature, T_{max}, and dissipated energy, E, predicted by the above relations, are given as a function of time, for fixed values of electrodes geometry, spark gap and electrical parameters. Moreover, two typical temperature profiles obtained with different gap/radius ratios are shown in Fig. 3.

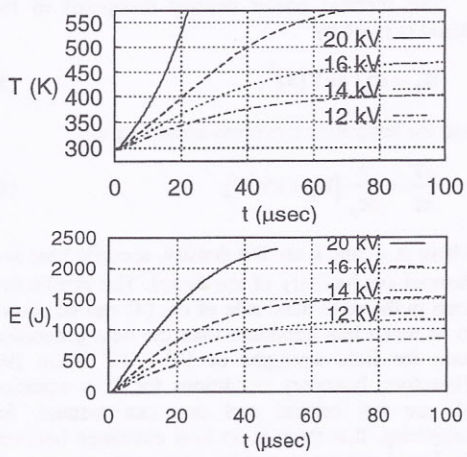

Fig. 2. Maximum temperature T_{max} and dissipated energy E as a function of time, for four values of charge voltage V_0. Gap distance: 1 cm, electrode radius: 1 cm, capacitance: 12 μF, inductance: 2.5 μH. Initial temperature: 296 K.

To validate the model, electrical and acoustical measurements were taken during the discharge of the paraboloidal sparker-based source at IDAC. The experimental apparatus consisted of a laboratory tank with dimensions 1 m by 0.64 m and a depth of 0.66 m. The paraboloidal source was positioned horizontally, and a 180 kHz bandwidth hydrophone was placed along the paraboloid axis. The liquid was fresh water with added sodium chloride, with a salinity of 3.4%. The electrostatic energy was supplied by a high-voltage generator (2250 Volt) charging a capacitor bank whose capacitance could

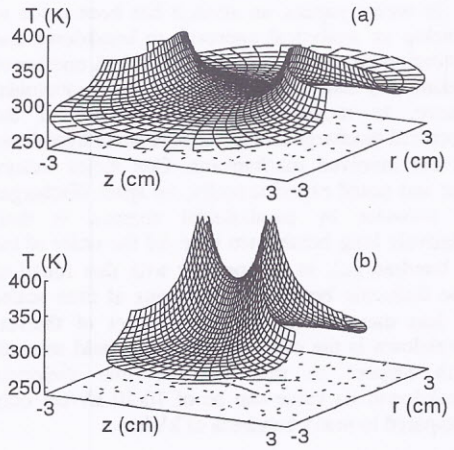

Fig. 3. Temperature profiles in the plane of cylindrical coordinates {r,z} after t = 3.5 ms for two different gap distances: 14 mm (a) and 8 mm (b). Electrode radius: 5 mm, charge voltage: 2250 V, capacitance: 360 μF, inductance: 2.5 μH. Initial temperature is 293 K. The curves in the base plane indicate the projections of the isothermal lines $T = T_{vap}$ = 373 K.

be varied in the range 40 - 360 μF. An auxiliary air spark gap was used to trigger the discharge. Particular care was taken for voltage and current measurements: voltage was measured directly across the two hemispherical tips of the electrodes excluding the inductive load of the connecting wires. A properly designed Hall effect detector was used to measure the current and, at the same time, to have a de-coupling between voltage and current wires. In this way, it was possible to verify that voltage and current are in phase during the plasma discharge, indicating that the spark gap behaves essentially as a purely resistive load. The total circuit inductance was kept to a minimum and estimated to be 2.5 μH, being essentially that of the cables from the capacitor bank to the sparker. Theoretical curves computed using equations (2), (4), (6), and (7) were compared with experimental data of voltage and current measured across the electrode gap. Fig. 4 is one of a series of similar plots [15] showing voltage and current as a function of time up to the observed breakdown time, for different values of hemispherical electrode radius and gap distance (In this case R = 5 mm, d = 4mm). The comparison generally shows a good agreement between theoretical and experimental data. The major differences were noted from the current values for cases with the smaller gap distance, where the deviation is possibly due to an alteration of the liquid chemical properties after several sparks, giving an actual higher conductivity. This is expected to be more evident in cases where a smaller portion of liquid is exposed to the electric field: indeed, the deviation is greater for both the smaller R and d.

A confirmation of the validity of the energy model arises from the comparison of the predicted

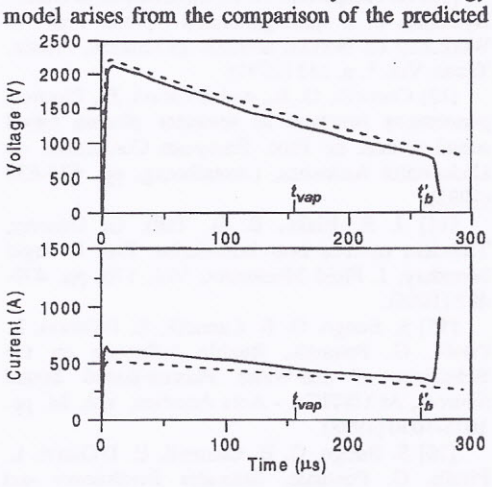

Fig. 4. Voltage and current as a function of time during the prebreakdown discharge: theoretical model (dashed line) and experimental data (solid line). Electrode radius: 5 mm, gap distance: 4 mm. Charge voltage: 2250 V, capacitance: 80 μF.

time required for liquid vaporization with the experimental breakdown time. Vaporization time is defined as

$$T_{\max}\left(t_{\text{vap}}\right) = T_{\text{vap}}, \tag{8}$$

where the standard value T_{vap} = 373 K may be assumed. A simple way to estimate the theoretical breakdown time t'_b is to continue the vaporization model until the vaporization temperature is reached at the midpoint between the electrodes, where the field strength and temperature are the lowest along the electrode gap. When this happens, a vapour channel with substantially lower density and higher electrical conductivity develops, leading to plasma generation and breakdown. In Fig. 4, two vertical segments represent the predicted t_{vap} and t'_b: these values are in good agreement with the observed breakdown times in the experimental curves.

4. Discussion

The above model suggest that electrical breakdown and subsequent thermal cavitation in a conducting liquid such as seawater can be described by a simple model of Joule heating with a temperature dependent electrical conductivity. It is proposed that breakdown mechanism is essentially that of a discharge in a low-density, highly conductive vapour, and that a sufficient amount of energy has to be delivered to the liquid in order to vaporize it and allow the discharge to take place in a gaseous phase. The electrical parameters of the discharge circuit may influence the time rate of the energy transfer, yielding low-power or high-power discharges. As a result, vaporization and breakdown may be slower or faster even with the same applied voltage. Discharges with a lower voltage and higher capacitance source may be equivalent to higher voltage discharges, only with a longer time scale.

From an analysis of plots in Fig. 2, it can be seen that the energy curves reach asymptotically their limiting value $CV_0^2/2$, and a critical temperature Tvap is reached when a given energy has been dissipated, defined as

$$E_{vap} = \int_0^{t_{vap}} I(t)\,V(t)\,dt. \tag{9}$$

If the energy available in the source does not exceed E_{vap}, regardless of the initial applied voltage, the discharge proceeds with no vaporization and subsequent breakdown. If the available energy is greater than E_{vap}, but not sufficient to raise the temperature at the gap midpoint above T_{vap}, vaporization (i.e. bubble growth and collapse) may take place, This is in agreement with experimental results [10].

The same can happen when the geometry of the electrodes does not allow high values of field strength over an extended region, that is for large electrode radius or gap distance. It can be pointed out from an inspection of the plots of Fig. 3 that increasing the gap distance over $d = R$ the temperature rise is greatly reduced, which suggests that there is a limiting value for d, beyond which the source ability to deliver energy to the liquid is greatly reduced. On the other hand, if d is small compared with R, the discharge may take place largely in vapour with little dissipated heat due to the high electric conductivity. In this case, the potential energy left in the source at $t = t_{vap}$ is not used for further heating of the liquid, but oscillates according to the usual *RLC* law between the capacitive and the inductive component of the load. Therefore, it seems reasonable to suppose that to optimize the efficiency of energy conversion into acoustical pressure, the vaporization should be reached when almost all the available energy has already been dissipated into the liquid.

For a fixed gap distance d, the model shows that the vaporization mechanism is optimal if the electrode radius R is smaller by approximately a factor of 2/3. If this condition is met, during the first stage of the discharge most of the heating is produced near the electrode surfaces, where the temperaturegradient is larger, which implies a faster growth rate for the vaporized regions towards the midpoint of the gap. If one relates the probability of a breakdown event to the temperature reached after a fixed time at the midpoint along the gap distance, an optimal value for R can be obtained once the gap distance d is given, for which a maximum temperature is attained. For smaller values of R the heating is highly localized near the electrodes, which could possibly imply some thermal and electrical insulation effects due to the gas layer surrounding the surfaces. For larger values of R more liquid is exposed to the electric field inside the gap, and the local value of field strength is lower, which implies that the heating process is less efficient.

References

[1] M. S. Plesset, A. Prosperetti, Bubble dynamics and cavitation, Ann. Rev. Fluid Mech. (9), pp. 145-185 (1977).

[2] G. B. Cannelli, E. D'Ottavi, Method of high-resolution sea bottom prospecting and tuned array of paraboloidal electroacoustic transducers to carry out such method, Japan Patent N. 5-505235 (August 5, 1993), USA Patent N. 5,398,217 (March 14, 1995), Canadian Patent N. 2,065,457 (July 14, 1998).

[3] G. B. Cannelli, E. D'Ottavi, L. Pitolli, G. Pontuale, Advances in the technology of paraboloidal sparker-based sources: Imaging of underwater objects using bubble implosion as the acoustic source, in Proc. 4th European Conference on Underwater Acoustics, Rome, pp. 407-412 (1998).

[4] A. P. Alkhimov, V. V. Vorob'ev, V. F. Klimkin, A. G. Ponomarenko, R. I. Soloukhin, The development of electrical discharge in water, Sov. Phys. Dokl. 15 (10), pp. 959-961 (1971).

[5] E. V. Yanshin, I. T. Ovchinnikov, Yu. N. Vershinin, Optical study of nanosecond prebreakdown phenomena in water, Sov. Phys. Tech. Phys. 18 (10), pp. 1303-1306 (1974).

[6] E. V. Yanshin, I. T. Ovchinnikov, Yu. N. Vershinin, Mechanism of the pulsed electrical breakdown of water, Sov. Phys. Dokl. 19 (2), pp. 95-96 (1974).

[7] I. M. Gavrilov, V. R. Kukhta, V. V. Lopatin, P. G. Petrov, V. Ya. Ushakov, Impulsive-discharge formation in water, Soviet Physics Journal 32, pp. 74-78 (1989).

[8] N. P. Mel'nikov, G. A. Ostroumov, M. Yu. Stoyak, Formation of electrical breakdown in aqueous sodium chloride solutions, Sov. Phys. Tech. Phys. 9 (5), pp. 730-733 (1964).

[9] V. G. Zhekul, G. B. Rakovskii, Theory of electrical discharge formation in a conducting liquid, Sov. Phys. Tech. Phys. 28 (1), pp. 4-8 (1983).

[10] A. H. Olson, S. P. Sutton, The physical mechanism leading to electrical breakdown in underwater arc sound sources, J. Acoust. Soc. Am. 94 (4), pp. 2226-2231 (1993).

[11] G. B. Cannelli, E. D'Ottavi, A. Prosperetti, Bubble activity induced by high-power marine sources, in: Proc. of OCEANS '90, Washington DC, pp. 533-537 (1990).

[12] A. Prosperetti, G. B. Cannelli, E. D'Ottavi, Dynamics of a spark-generated bubble, Proc. of Workshop on thermal acoustic generation, Austin, Texas, Vol. 1, p. 133 (1991).

[13] Cannelli, G. B., and D'Ottavi, E., Physical phenomena involved in seawater plasma based sound source, in: Proc. European Conference on Underwater Acoustics, Luxembourg, pp. 635-638 (1992).

[14] J. R. Blake, B. B. Taib, G. Doherty, Transient cavities near boundaries. Part 1. Rigid boundary, J. Fluid Mechanics, Vol. 170, pp. 479-497 (1986).

[15] S. Buogo, G. B. Cannelli, E. D'Ottavi, L. Pitolli, G. Pontuale, Bubble Influence on the Behaviour of Sea-Water Plasma-Based Sound Sources, ACUSTICA - Acta Acustica, Vol. 84, pp. 1025-1030 (1998).

[16] S. Buogo, G. B. Cannelli, E. D'Ottavi, L. Pitolli, G. Pontuale, Seawater Breakdown and Bubble Generation in Marine Sparker Based Sound Sources, in: Proc. 4th European Conference on Underwater Acoustics, Roma, pp. 119-124 (1998).